Applied Energy xxx (xxxx) xxx

Contents lists available at ScienceDirect

Applied Energy

journal homepage: www.elsevier.com/locate/apenergy

Opportunities for wave energy in bulk power system operations

Kerem Ziya Akdemir [a,b,1], Bryson Robertson [a,c], Konstantinos Oikonomou [a], Jordan Kern [d], Nathalie Voisin [a,e], Sarmad Hanif [a], Saptarshi Bhattacharya [a,*]

[a] Pacific Northwest National Laboratory, Richland, WA, United States of America
[b] Department of Civil, Construction, and Environmental Engineering, North Carolina State University, Raleigh, NC, United States of America
[c] School of Civil and Construction Engineering, Oregon State University, Corvallis, OR, United States of America
[d] Department of Industrial and Systems Engineering, North Carolina State University, Raleigh, NC, United States of America
[e] Department of Civil and Environmental Engineering, University of Washington, Seattle, WA, United States of America

ARTICLE INFO

Keywords:
Production cost modeling
Marine renewable energy
Wave energy
Electricity market
Power system operations
Contingency analysis

ABSTRACT

Wave energy resources have high, yet largely untapped potential as candidate generation technology. In this paper, we perform a data-driven analysis to characterize the impact of wave energy integration on bulk-scale power systems and market operations. Through data-driven sensitivity studies centered on an optimization-based production cost modeling formulation, our work characterizes the inflection point beyond which wave integration starts impacting power system operations, considering present day transmission infrastructure. Furthermore, our analysis also considers the joint effects of wave energy integration and system-wide transmission expansion. Finally, potential resilience scenarios such as wildfire-driven transmission contingencies and heat wave events are investigated, whereby the contributions of grid-integrated wave energy in alleviating the effects of the resilience events are analyzed. As our demonstration test bed, we consider a reduced-order network topology for the U.S. Western Interconnection with wave energy generation integrated at carefully selected sites across the coastal areas of Washington, Oregon, and northern California. Our results indicate that over a representative year of operations, wave energy integration systematically reduces locational marginal prices (LMPs) of energy and price volatility, especially during periods of high wave resource availability (winter months for the U.S. west coast). Average, maximum, and minimum of hourly LMPs over a typical year of operation was reduced by 2.95, 51.28, and 1.13 $/MWh respectively (over a baseline scenario with no wave energy integration), when the selected network model had a total of 5000 MW wave power installed capacity during the representative year of study. The effects of wave energy integration can remain localized with existing transmission infrastructure (identified to be most pronounced in the Pacific Northwest region in the example we studied). However, with concurrent transmission expansion, the impacts of wave energy integration are likely to have a higher geographical spread. Our results also indicate that wave energy may be able to assist power system operations during resilience events such as major transmission contingencies and heat wave events, although such benefits might be dependent on factors such as proximity of affected area to wave resources, availability of adequate resource potential and adequate transmission capacity.

1. Introduction

Renewable energy integration has been deemed critical for ensuring a sustainable and decarbonized future energy landscape [1,2]. As grids are decarbonized, grid operators need to come up with alternative methods to ensure reliability during normal operations as well as during extreme weather events [3]. In this context, it is not only essential to develop key technologies that facilitate seamless and efficient integration of existing and technically advanced renewable generation resources (such as wind and solar), but also important to investigate relatively newer modes of renewable energy generation [4], that may have potential for added benefits. Marine energy resources (including wave, tidal, and ocean currents) are one such group of resources that have significant potential to emerge as effective clean generation alternatives [5–7].

Authors in [8] show that at a worldwide scale, ocean waves have a potential reserve of 2 TW of power, which is approximately equal to the global energy demand. For the United States (U.S.) alone, the projected wave energy content across the continental coastline is 2.64

* Corresponding author.
E-mail address: saptarshi.bhattacharya@pnnl.gov (S. Bhattacharya).
[1] The work was done during the author's internship at Pacific Northwest National Laboratory.

https://doi.org/10.1016/j.apenergy.2023.121845
Received 30 May 2023; Received in revised form 29 July 2023; Accepted 25 August 2023

TWh/year [9], which is equal to approximately 65% of the country's total annual energy demand [10,11]. Compared to other renewable resources such as wind and solar, some forms of marine energy resources, such as wave energy and tidal energy are more periodic, persistent, and predictable [12,13]. Researchers have studied the possible advantages of including wave and tidal energy within the generation portfolio on power system operations [7,14,15]. Specifically, wave energy is observed to be the most scalable among marine energy resources and its integration in bulk power system operation has proven potential to reduce balancing requirements, improve effective load carrying capabilities, and also improve operational reliability and resiliency [12].

As marine energy is a relatively nascent technology when compared to wind and solar, a substantial body of work has focused on assessing its technical suitability [16–19] economic viability [20,21] and identifying development sites with optimal resource potential [22–24]. Although there has been a body of work investigating the possible impacts on power system operations, these analyses have been mostly performed in grid-abstracted settings that do not model power system specifics in detail or have focused on grid interconnection issues at the device/converter level [25–28]. Additionally, the impact of wave power in transmission-constrained systems has been studied in [5], where authors posited that wave energy reduces the energy demand from other sources of generation. Even with this related body of work, there remains a need to further understand the value proposition of wave energy in continental-scale bulk power system operations, specifically, we need to quantitatively characterize its contribution to day-to-day operations as measured with key performance metrics such as operational and market dynamics, as well as the contribution during extreme events.

In this paper, we investigate the potential impact of integrating marine energy-based generation resources on bulk-scale power system operations. Owing to considerable high-quality wave-based resource availability on the western coast of continental United States, we selected a reduced order network model of the U.S. Western Interconnection as our test bed in this work [29]. This power system model was equipped with wave energy generation at key points across the western coast of the United States (the states of Washington, Oregon, and California). Subsequently, we study the impact of the assumed wave generation on power system operations through an optimization-based unit commitment/economic dispatch (UC/ED) formulation, under several different types of operating conditions. Please note that the choice of wave as the studied resource is driven by the inherently scalable nature of wave energy technology. Other marine energy technologies such as tidal energy are largely restricted to localized impacts or are not as scalable as wave, and are hence not considered in this study.

The main contributions of our work are listed as follows. Firstly, to the best of our knowledge, this is the first-of-its-kind study to consider the impact of wave generation on bulk power system operations. Key insights are presented on how wave energy can bring down energy prices across critical demand locations across the power system. Secondly, our analysis also characterizes the spatial distribution of the benefits stemming from the aforementioned wave integration and analyzes transmission upgrade scenarios that can aid in translating the benefits of wave integration over a greater geographical spread. Thirdly, our work also investigates the role of wave energy on system operations under extreme weather events like heat waves and power system contingencies, and comments on the applicability of wave energy at scale to address power system resiliency issues.

The rest of the paper is organized as follows. Section 2 provides a description of the grid operations model and marine energy (wave) generation data used for this study. Section 3 provides a description of the study scenarios along with the details of the corresponding experimental designs. All numerical results, including model validation and results from the designed experiments (as noted in Section 3) are presented in Section 4. Finally, we provide concluding remarks followed by limitations and future research directions in Section 5.

2. Methods

In this section, we provide a brief description of the unit commitment and economic dispatch (UC/ED) model used for simulating grid operations. Note that the main objective of this paper is to employ this UC/ED framework to investigate the key opportunities that can be explored by integrating wave energy resources at scale to bulk-scale power system operations. Therefore, a model suitable for conducting experiments has to (a) represent power system operations for a realistic bulk power system and (b) have a geographical area of coverage that has sufficient good-quality wave resources. For the US, the western seaboard has some of the best wave resources in the country [30,31], a balanced mix of major load centers located in close proximity to the coast as well as in more inland areas, away from the coast. Thus, we have selected the U.S. Western Interconnection as the candidate power system model in our study. In order to study the impact of marine renewable energy (MRE) resources on the overall U.S. Western Interconnection in a scalable manner, a systematic model reduction is performed to design an equivalent reduced topology network for the entire U.S. Western Interconnection. Criteria for selecting node locations in the reduced topology are subsequently described. Lastly, an overview of modeling the MRE resources is presented.

2.1. UC/ED model formulation

In this study, an open-source production cost modeling framework for the U.S. Western Interconnection called GO WEST [29] is used as a baseline to create the specific test case for wave energy integration.

Spanning over 4.66 million square kilometers, the U.S. Western Interconnection encompasses several U.S. states, Canadian provinces, and some parts of Baja California in Mexico. It provides electricity to approximately 80 million people [32]. In 2018, the total nameplate capacity of all power plants in the U.S. Western Interconnection was 258,200 MW. The capacity mix is dominated by natural gas (38%) and hydroelectric power plants (27%), and they are followed by coal, nuclear, wind, and solar power plants [33].

GO WEST accounts for the grid operation in only the U.S. states of Western Interconnection, which include California, Oregon, Washington, Idaho, Nevada, Arizona, Utah, Wyoming, Montana, Colorado, and New Mexico. It is a Python-based software where the UC/ED mathematical optimization is solved by the solver Gurobi. Note that while the UC problem typically entails solving a mixed-integer linear program (MILP), the ED version is a pure linear program (LP). With GO modeling framework, users can choose between LP and MILP for their specific research study.

The model's objective is to minimize the total cost of providing necessary electricity to meet the total energy demand across the entire power system, subject to constraints that restrict the generator commitment and dispatch decisions such as generator ramp rate limits, maximum generator capacities, and minimum up and down times. There are also other constraints like thermal limits of the transmission lines and nodal power balances. The model operates on a user-defined 24-hour horizon and the temporal resolution of the model outputs is hourly.

Decision variables of the model consist of on/off status and electricity generation from each generator, voltage angle at each node, and power flow on each transmission line. There is one slack generator at each node that has an extremely high marginal cost of generation and is used only as a last resort. Slack generators are often used to detect loss of load events at any point in time and account for power imbalances arising due to such events [34]. Model outputs include the generation schedule of each generator, power flow on each transmission line, locational marginal prices (LMP) at each node (typically characterized by the dual of power balance constraint at any node), voltage angles, and loss of load events at each node.

Scheduling and dispatch of thermal generators, like natural gas and coal, depends on several inputs like heat rates, fuel prices, and variable operation and maintenance costs as well as generator-related constraints. In the GO WEST model, nuclear power plants are considered as a *must-run* resource, except when there is a planned or forced generator outage. On the other hand, renewable generators are modeled differently. Historical hourly generation from solar and wind generators is gathered from EIA-930 dataset [35] at the balancing authority scale and is remapped to the reduced nodal scale. Hourly available solar, wind, and wave generation at each node are provided as input to the model, which then decides how much of the available solar, wind, and wave power to dispatch. This means that the model might choose to curtail renewable generation depending on the grid conditions even though the marginal cost of renewable generators is low. On the other hand, a different approach is followed to model hydropower generators. Historical weekly hydropower datasets include generation targets as well as hourly minimum, hourly maximum, and daily maximum fluctuations. The generation targets are based on a modified version of EIA-923 dataset [36], further downscaled based on USGS flows [37]. The hydropower is dispatched hourly (with an operational daily maximum flow constraint) based on the power grid needs.

GO WEST uses a synthetic 10,000-node representation of U.S Western Interconnection [38,39]. Given that running a model of this scale would be both time- and resource-intensive, researchers often make use of simplified, reduced-topology model versions of detailed power systems. In this regard, GO WEST allows users to select different number of nodes suitable for their studies, type of mathematical formulation (LP, i.e., only economic dispatch versus MILP, i.e., combined unit commitment and economic dispatch), transmission line scaling factors as well as hurdle rate scaling factors.

- **Number of nodes:** Users of GO WEST can select the number of nodes to retain from 10,000 nodal topology of the U.S. Western Interconnection (TAMU network). In this study, we selected 134 nodes to represent grid operations in Western Interconnection (see Section 2.2 for more details).
- **Mathematical formulations:** Although GO WEST allows both UC and ED formulations as discussed earlier, in this paper, we selected the LP version (i.e., economic dispatch only) owing to its reasonable run times and comparable degree of accuracy, when compared with the results of the corresponding MILP (i.e., unit commitment) formulation [29].
- **Transmission line capacity scaling factors:** GO WEST determines the transmission line locations and thermal capacities for any reduced network automatically by utilizing a network reduction algorithm [29]. However, additional calibration of transmission line capacities is necessary since there might be inconsistencies in the line limits calculated by the network reduction algorithm. In this study, thermal limits for congested lines over a pre-selected threshold were scaled up by a factor of 500 MW. All other lines retained their original thermal limits as prescribed by the network reduction algorithm.
- **Hurdle rate scaling factors:** A hurdle rate is defined by the cost of transferring 1 MW of power between two balancing authorities (BAs). A balancing authority oversees the electrical balance in its region. There are 28 BAs in GO WEST model. Original hurdle rates between BAs are gathered from Western Electricity Coordinating Council (WECC) Anchor Data Set [40]. GO WEST model allows scaling hurdle rates up and down by user-defined percentages. In this study, we used the hurdle rates as reported by WECC and did not use hurdle rate scaling factors.

2.2. Nodal topology selection

In this section, we detail the steps of generating the 134-node reduced order model from the 10,000 parent topology. The metrics chosen for validation are (a) zonal LMPs and (b) system-wide generation portfolio composition (see Section 4.1 for numerical validation of the selected reduced topology model). Detailed node selection steps are enumerated below:

- Ten nodes throughout the Western Interconnection are selected specifically to host wave generation resources. Selection of the wave energy generator nodes is consistent with resource potential (wave power density), regions with existing infrastructure, and transmission capabilities across the western coast of continental U.S. [41]. Specifically, two of these nodes are located in Washington, four in Oregon, and the last four nodes are placed in northern California. Note that in this study, we use wave energy as the only MRE resource since wave is considered to be the most scalable of the MRE resources [12,42].
- After selecting the wave generator nodes, nodes with the highest demand in each of the 28 balancing authorities (BA) are also added to the custom topology to represent high-load areas (e.g., cities) - this ensures at least one node in each state is selected.
- The remaining 96 nodes are uniformly divided into three categories; demand nodes, generation nodes, and transmission nodes. During the selection process of these nodes, a relatively higher priority is given to coastal states (Washington, California, and Oregon) to adequately capture wave power transmission ability to more inland nodes. Furthermore, demand and generation nodes are prioritized in proportion to their associated demand quantities and generation capabilities respectively. For transmission, the nodes having access to lines higher than 345 kV are prioritized.

Through the nodal selection procedure, two different distance thresholds are used. These thresholds make sure that the selected nodes are separated by a certain distance. We used a 30 km threshold while selecting a node in each BA, otherwise, an 80 km threshold is used elsewhere. The reason for using a 30 km threshold during node selection in each BA is to include at least one node in BAs that has a smaller service area. This approach allows a more dispersed topology while retaining the most important nodes (major demand centers, generation options, and transmission corridors). Fig. 1 serves as a comparison of 10,000 nodal topology and 134 nodal topology we created for this study.

2.3. Wave energy modeling

The development of the necessary wave power (energy) generation characteristics for integration into the GO WEST model representation of the Western Interconnect is dependent on two major factors; the gross resource availability along the western seaboard of the U.S., and the conversion efficiency of the wave energy converters (WECs) from this gross resource into a usable net electrical power generation. A consistent, time-coherent, and well-validated dataset of the offshore wave energy gross resource characteristics is required to ensure the wave energy generation is well represented. Two data streams were used in this analysis.

Firstly, numerical wave propagation model outputs from a Simulating Waves Nearshore (SWAN) model [43] were utilized for the integration scenarios in 2019 (i.e., the representative year of study). This data included details on the significant wave height and wave energy period, as per International Electrotechnical Commission specifications [44]. This data is publicly available from the National Renewable Energy Laboratory's Marine Energy Atlas [45]. Secondly, higher temporal resolution data which is time coherent with the respective

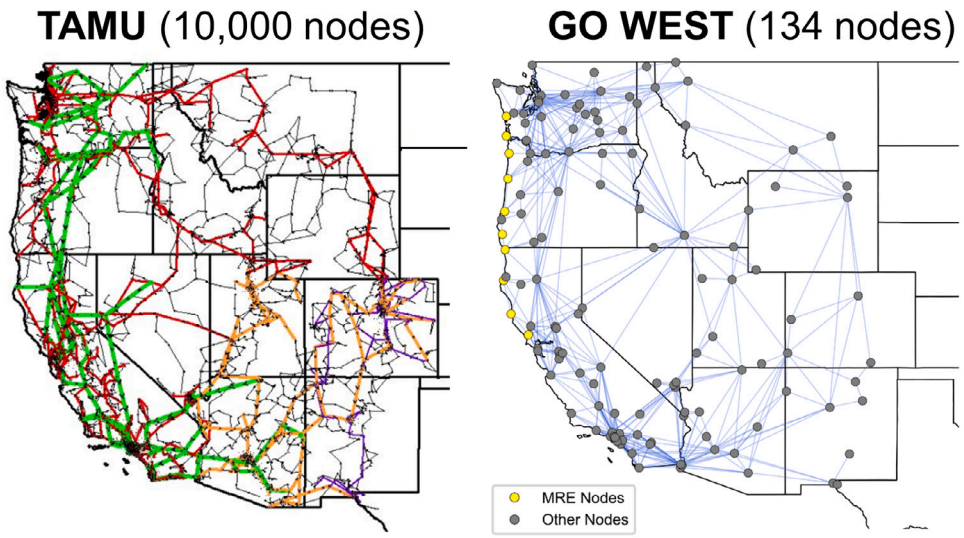

Fig. 1. Comparison of the nodal topologies of the 10,000 node WECC representation (TAMU) and the reduced order 134 node representation developed for this study.

demand data was needed for simulating wave power during California heat wave in 2020 (see Section 3 for more details on these scenarios). The necessary gross wave resource data for 2020 was harvested from in-situ device measurements, which are stored on National Data Buoy Center database for the following buoys: 46013, 46014, 46022, 46027, 46029, 46041, 46050. In order the quantify the conversion efficiency of the WECs, it was important to ensure that the results of this study were specific technology-agnostic. The conversion efficiency is needed to properly represent both existing WEC designs but also provide a reliable representation of possible future technologies. Utilizing the methodology developed by Robertson, et al. [46], the conversion efficiency of the WECs was represented by a two parameter surface; with dependencies on both significant wave height and energy period. To ensure complementarity with existing renewables (i.e., wind and solar), the conversion efficiency surface includes 'cut-in' and rated power limits. Finally, the MRE generation profiles were developed by assessing the significant wave height and wave energy period at each location, for each hour, and identifying the appropriate conversion efficiency from the generic WEC representation. Normalized wave power outputs for the representative year of study (2019) at the 10 aforementioned locations (for locations, see Fig. 2) selected for this study are shown in Fig. 3.

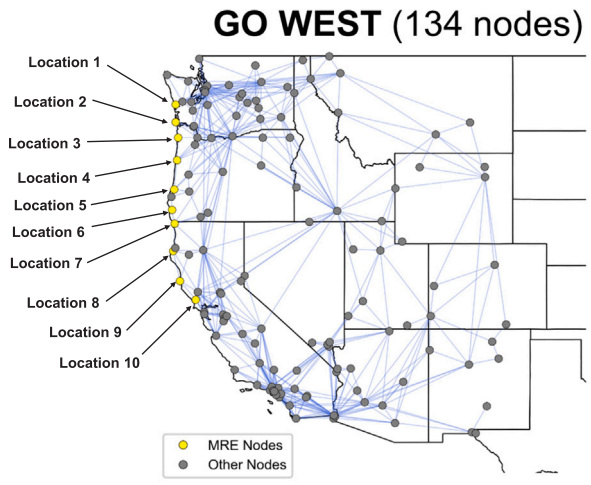

Fig. 2. Locations of the selected nodes where wave energy-based generation is considered for installation.

3. Study scenarios and experimental design

In order to investigate the impacts of integrating MRE resources (wave energy) on bulk power system operations, a variety of scenarios were generated to help identify opportunities and challenges. The contribution of any new technology to bulk power grid operations is a function of the installed capacity. For a robust evaluation of the value proposition of wave energy to the contemporary grid of 2019 (our representative case study in this paper), eight different wave energy capacity penetration scenarios are considered, with installed wave capacities of 10 MW, 20 MW, 50 MW, 100 MW, 200 MW, 300 MW, 400 MW, and 500 MW in each wave generation node. The operational and market impacts are analyzed both spatially and temporally.

As the integration of wave energy increases in the scenario, transmission constraints might limit the value proposition. Thus, we also study an alternate scenario where we increase the transmission line capacities equally by +500 MW throughout the Western Interconnection for each of the aforementioned wave energy penetration scenarios. The two sets of 8 scenarios provide a realistic evaluation of the potential contribution of wave energy to key performance metrics of the bulk power system, the first one relying on the 2019 infrastructure and the second set requiring an investment in transmission upgrades to achieve the full potential of the new technology.

Another opportunity of wave energy is to support power grid resilience. Specifically, we use two stress tests which are an artificial wildfire in August 2019 and a historical heat wave in August 2020, as described in Sections 4.4 and 4.5 respectively. Our selection of the wildfire event has been motivated by the observation that natural hazards (including forest fires) have significantly impeded power system operations in recent years [47], with wildfire-driven contingencies being of particular prominence in the Oregon/northern California region [48]. Lastly, we analyzed the value of having wave power during the historical California heat wave that occurred between August 14, 2020 and August 19, 2020. This specific heat wave led to significant LMP spikes in California due to high electricity loads driven by extreme space cooling needs. During this extreme event, California Independent System Operator (CAISO) had to implement rotating outages to prevent more damage to the bulk electricity grid [49].

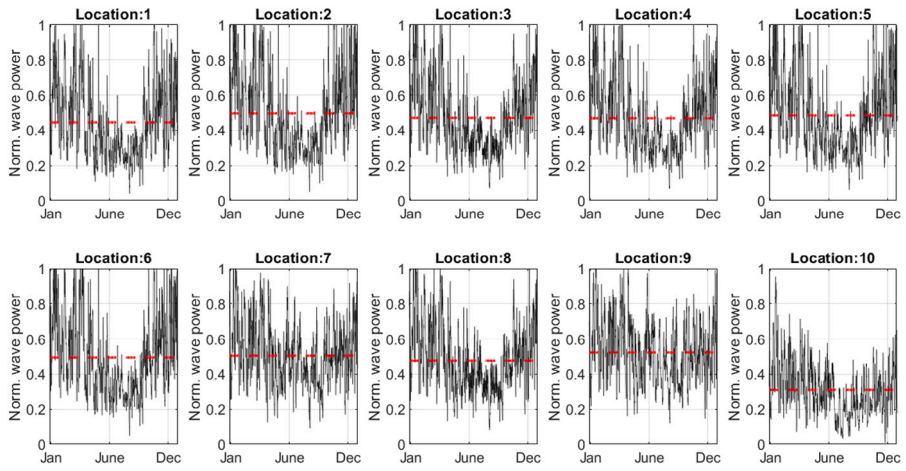

Fig. 3. Normalized wave power outputs for the 10 selected locations, along with their yearly normalized average values (shown in red dotted line).

4. Results and discussion

4.1. Model validation

Prior to detailed investigations into the impact of wave energy, it is important to ensure the baseline model well represents historical characteristics. The selected model version is validated by comparing simulated LMPs and generation mix with historical data in 2019. The left side of Fig. 4 illustrates the LMP validation, which includes a time series comparison of simulated LMPs to historical LMPs in 2019. Daily LMP data for pricing hubs are calculated by taking a demand-weighted average of simulated LMPs at each node within each pricing hub. Relevant R^2 and root mean square error (RMSE) is calculated for each pricing hub. From Fig. 4 (left-hand side plot), we can conclude that our version of the GO WEST model can capture LMPs appreciably well in all pricing hubs.

From the second plot (right-hand side) of Fig. 4, we can infer that our model appreciably captures solar, wind, hydro, and nuclear generation. However, the over-utilization of natural gas plants more than historical data can be partly attributed to the inability of importing electricity from outside the U.S. (e.g., Canada). Therefore, our model has to generate more electricity from natural gas power plants to ensure adequate power balance. Another reason can be the lack of granular fuel price data for each balancing authority, which can impact the subsequent merit order dispatch in the ED solution. Nevertheless, even with the aforementioned artifact, the selected topology captures the major generation mix in the U.S. Western Interconnection with reasonable accuracy.

4.2. Impacts of integrating different wave energy capacities

In this study, we analyze the results of the 8760-hour economic dispatch with the selected topology (assuming 2019 operations) under eight different wave energy penetration scenarios where the installed capacities of wave energy in each MRE generator node were assumed to be 10 MW, 20 MW, 50 MW, 100 MW, 200 MW, 300 MW, 400 MW, and 500 MW. In these simulations, the specified wave energy capacity is integrated into every MRE node simultaneously by the same amounts.

Hourly average, standard deviation, maximum, and minimum of LMPs for each scenario is listed in Table 1, which reflects the prices for overall Western Interconnection. Note that we calculated hourly LMPs for the whole Western Interconnection by taking a demand-weighted average of simulated LMPs at each node. Even though lower wave energy capacities do not have a significant impact on the LMPs, after reaching 50 MW wave capacity, we start to observe LMP reductions. Integrating 100 MW wave power decreases average LMPs by 0.91 $/MWh whereas 500 MW wave power leads to a reduction in average LMPs by 2.95 $/MWh. Furthermore, wave power decreases price volatility by reducing the standard deviation of LMPs. Adding 100 MW and 500 MW of wave capacity to each node diminishes the maximum LMPs observed in 2019 by 16.85 and 51.28 $/MWh, respectively. Additionally, beyond 200 MW wave integration, even minimum prices start to decrease as well.

Table 1
Hourly LMP statistics for the whole Western Interconnection with and without wave energy integration in 2019.

Installed wave capacity per generator node (MW)	Average LMP ($/MWh)	Standard Deviation of LMPs ($/MWh)	Maximum LMP ($/MWh)	Minimum LMP ($/MWh)
0 (Baseline)	43.43	49.86	504.15	14.62
10	43.32	49.60	503.76	14.62
20	43.28	49.55	503.46	14.62
50	42.97	48.09	497.48	14.62
100	42.52	45.98	487.30	14.62
200	42.14	45.36	484.10	14.49
300	41.74	45.04	482.09	13.98
400	41.22	43.89	467.76	13.88
500	40.48	41.41	452.87	13.49

Subsequently, we now study the temporal characteristics of the LMP reduction in Fig. 5. We observe that before 50 MW wave power, there are minimal changes in LMPs when compared to the baseline configuration. After the 50 MW threshold, LMP reductions mostly occur in February and especially in March. This timing can be attributed to wave power being a stronger resource in winter months [12]. Another likely contributing factor can be the higher-than-normal LMPs during the winter of 2019 due to supply constraints on natural gas and extremely cold temperatures [50]. As wave power capacity grows, LMP depreciation becomes more pronounced. Beyond 200 MW wave integration, price reductions are observed in late fall and spring as well, in addition to winter months.

In Fig. 6, we study the LMP reduction due to wave integration from a spatial viewpoint. Specifically, the reduction in LMPs in the individual nodes of our reduced topology model is plotted, from which we can clearly see that LMP reduction is more pronounced in the Pacific Northwest region (from coastal WA to northern CA), which is situated in close proximity to MRE generator nodes or has adequate transmission infrastructure for the benefits of wave generation to percolate inland.

Fig. 6 demonstrates as integrated wave power capacity grows, the LMP depreciation also increases but only in a subset of nodes. Therefore, we can infer that if wave power integration is not accompanied by sufficient transmission infrastructure, the benefits of wave power will potentially remain localized.

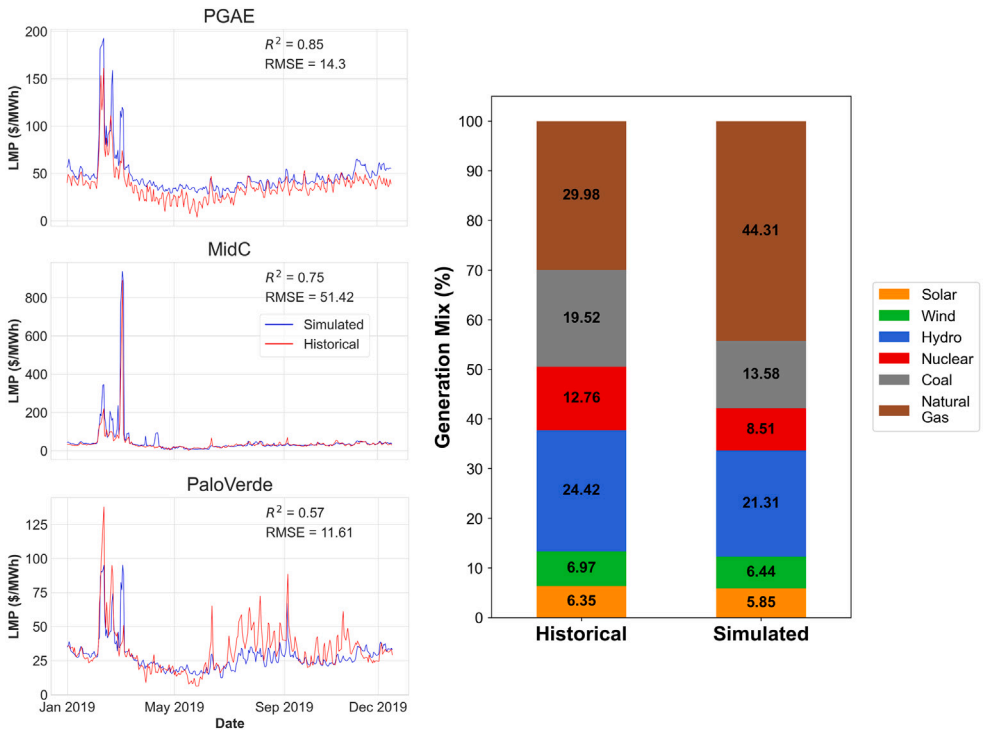

Fig. 4. (Left) Historical and simulated daily LMPs for Mid-Columbia (MidC), Southwest (PaloVerde), and Pacific Gas and Electric (PGAE) in 2019; (right) comparison of historical and simulated generation mix percentages for the whole Western Interconnection in 2019.

Table 2
Hourly LMP statistics for the whole Western Interconnection with and without wave energy integration in 2019. This table shows results for the case in which all transmission line capacities are additively scaled by +500 MW.

Installed wave capacity per generator node (MW)	Average LMP ($/MWh)	Standard Deviation of LMPs ($/MWh)	Maximum LMP ($/MWh)	Minimum LMP ($/MWh)
0 (Baseline)	33.98	15.44	158.11	16.36
10	33.96	15.42	158.11	16.36
20	33.94	15.42	158.16	16.36
50	33.87	15.38	158.18	16.36
100	33.76	15.33	157.1	16.36
200	33.57	15.22	156.72	16.2
300	33.37	15.06	155.59	16.17
400	33.15	14.9	155.43	16.17
500	32.93	14.77	155.18	16.17

4.3. Impact of concurrent transmission capacity expansion and wave energy integration

In this section, we repeat our experiments in Section 4.2 considering an increased transmission capacity (+500 MW) across all transmission lines in the reduced topology network. For this study, LMP statistics in 2019 for the overall Western Interconnection under each wave penetration scenario are listed in Table 2. Again, we calculated hourly LMPs for the Western Interconnection by taking a demand-weighted average of simulated LMPs at each node. Since improving transmission capabilities enables inland nodes to take advantage of cheap electricity produced by wave resources, the overall price depreciation is much smaller due to the spread of the benefits. Even with 500 MW wave power, average LMPs reduce only by 1.05 $/MWh. Although price volatility in terms of standard deviation, maximum and minimum prices reduce with the integration of wave power, the amount of change is much lower than in the earlier case where an expanded transmission infrastructure was not considered.

Temporal LMP differences resulting from wave energy integration under each scenario are illustrated in Fig. 7. No noticeable impact on the LMPs below 50 MW wave integration is observed, as was the case without transmission expansion. As wave power capacity grows, LMP reductions also increase and become dominant in February, which is also similar to our observation without transmission expansion in Section 4.2. In addition to winter months, LMP benefits from wave power start to emerge in late fall and spring after 200 MW integration case. In addition, higher LMP reductions occur between 7 PM and 8 AM since wave resources are more persistently available (at a relative scale when compared to wind and solar) during the night [12]. Lastly, when compared to Fig. 5, the boundary of LMP difference is narrower (i.e., maximum LMP reduction is lower) in Fig. 7 due to the higher spatial spread of wave energy integration impact.

From a spatial viewpoint, the LMP reduction effect is observed to be significantly more spread out over a wider geographical extent, thereby highlighting the benefits of concurrent transmission expansion in leveraging the benefits of wave energy. Fig. 8 verifies that wave power's positive impacts (e.g., LMP reductions) can reach inland nodes when coupled with transmission investments. On the other hand, LMP depreciation in most of the nodes becomes relatively lesser due to the benefit now spreading over a greater geographical region with increased transmission capabilities. In order to understand the scale of the wave power integration for this study, it should be noted that the total capacity of integrated wave power (5000 MW from the 10 wave energy generator nodes) corresponds to 1.9% of the total installed capacity in the U.S. Western Interconnection.

4.4. Impact of wave energy integration under resilience scenario: Wildfire contingency event

In this section, we analyzed the effect of including wave energy in the generation mix during a transmission line contingency (outage of major transmission lines) due to an artificial wildfire. Informed by wildfire statistics within the U.S. [51,52], we assumed an artificial wildfire that extends spatially from northern California to Oregon causing

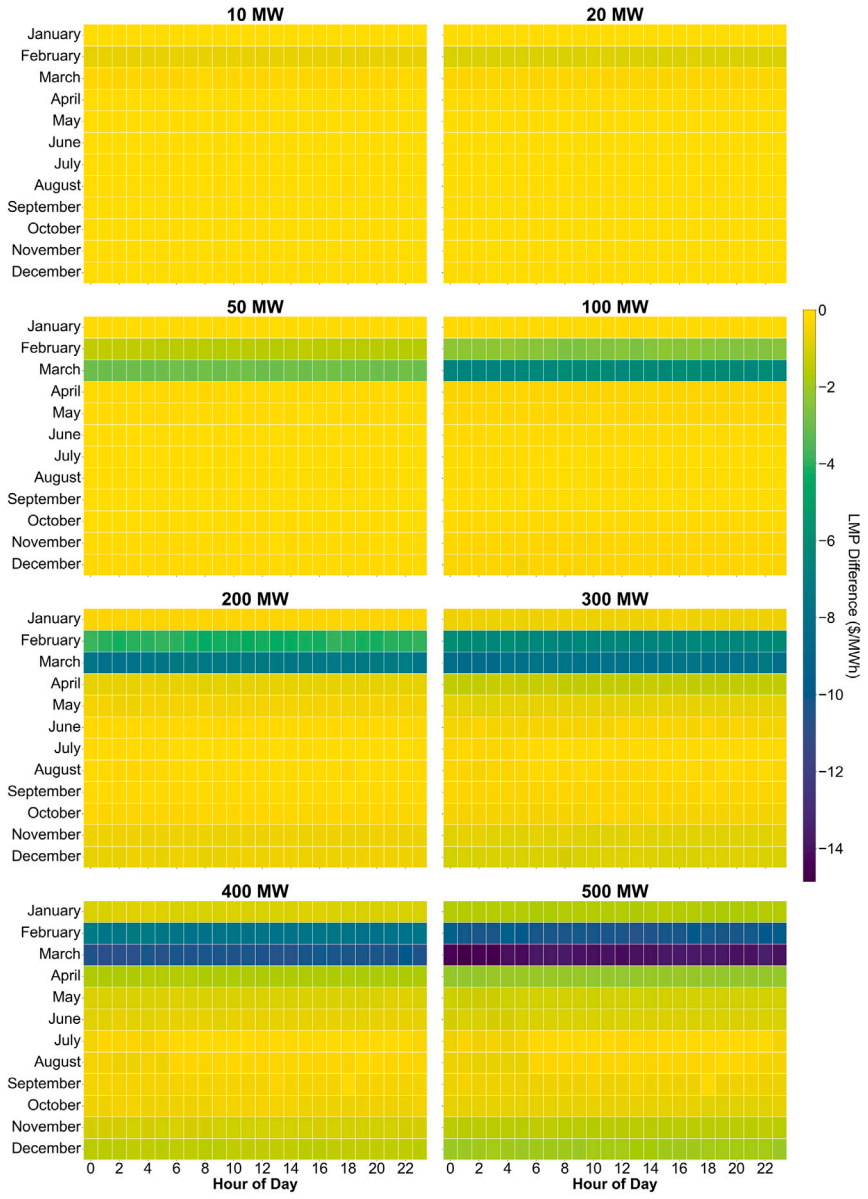

Fig. 5. Fluctuation map of LMP changes due to wave power integration for each scenario. LMP difference designates the change in LMPs between the baseline scenario (0 MW wave power) and each MRE scenario. Negative values show LMP decrease due to wave power integration. Each row shows the hourly profile of an average day in different months of 2019.

associated transmission line derating in the region. The choice of the event time (August 7th to August 14th, 2019) is guided by literature on identifying causative factors for wildfire inception events [53], historical 2019 hourly dry bulb temperatures, relative humidity, and wind speed data from Montague Siskiyou Airport). We assumed that the wildfire-driven line contingency duration is 1 week. In order to study the impact of having wave resources in the generation mix during these aforementioned line outage scenarios, we considered installed capacities of 100 MW and 500 MW of wave generation to every wave energy generator node and compared the results with the baseline case, where no wave resource was available.

Nodal LMP effects of having wave power in the generation mix during the simulated transmission line contingency event are illustrated in Fig. 9. When there is no wave power available, average LMPs in a majority of the nodes that are directly connected to transmission lines affected by the outage event spiked above 1000 $/MWh. This is because there was a supply shortfall in those nodes, which lead to unserved load events (reflected by high loss-of-load pricing). The price shock impact of the wildfire extends northwards up to some areas of Washington. However, with 500 MW wave power capacity at every wave energy generator node during the event, the nodal LMP spikes due to the wildfire event were observed to be alleviated to some extent.

It is crucial to track the hourly grid influences from MRE resources to comprehend the overall value of possible integration. Fig. 10 visualizes the average LMPs in line outage nodes as well as the total unserved load for each scenario (0 MW i.e., baseline, 100 MW, and 500 MW of wave power capacity). Although the LMP depreciation benefits of having 100 MW wave power capacity are relatively lesser, integrating 500 MW wave capacity leads to significant LMP reductions during the event. In line with this observation, 500 MW wave capacity integration was also observed to curb unserved load (i.e., loss of load events) in the 14 line outage nodes that are directly affected by the studied wildfire event.

Table 3 provides summary statistics for the whole Western Interconnection under each scenario. The wildfire event increased average LMPs throughout the Western Interconnection by 177.4 $/MWh under baseline conditions (no wave power). Integrating 100 MW and 500

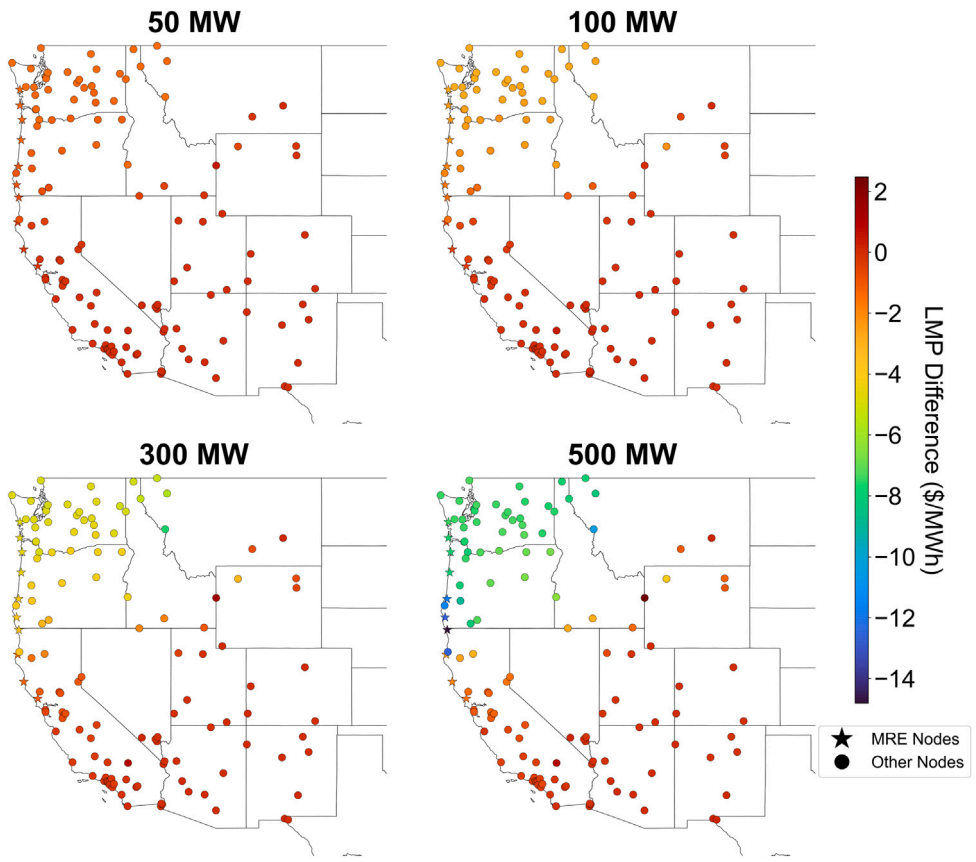

Fig. 6. Average nodal LMP changes due to wave power integration for four selected scenarios in 2019. LMP difference designates the change in LMPs between the baseline scenario (0 MW wave energy capacity) and each wave integration scenario. Negative values show LMP decrease due to wave power integration. Color designates the magnitude of average LMP change at each node. MRE nodes are shown with stars whereas other nodes are shown with circles.

Table 3
Summary statistics for the whole Western Interconnection during the contingency event in 2019.

Scenario	Avg. LMP ($/MWh)	Std. Dev. of LMPs ($/MWh)	Max. LMP ($/MWh)	Min. LMP ($/MWh)	Avg. Hourly Unserved Load (MW)
No wildfire	30.73	7.40	51.75	23.25	2.36
No wave power + wildfire scenario	208.13	40.89	321.22	129.55	789.56
100 MW wave power + wildfire scenario	200.49	33.67	290.24	129.54	733.67
500 MW wave power + wildfire scenario	166.57	39.07	284.01	99.02	535.45

MW wave power to every MRE node (i.e., 1000 MW and 5000 MW wave power in total across the entire U.S. Western Interconnection) led average LMPs to drop by 7.64 and 41.56 $/MWh, respectively. Wave power also reduces the price volatility by decreasing standard deviation, and maximum and minimum LMPs during the event. Even though 100 MW wave power integration does not change the minimum LMPs, increasing wave power capacity further to 500 MW reduces the minimum LMPs by more than 30 $/MWh. Lastly, the wildfire event (and subsequent transmission line outages) was observed to have increased the average hourly unserved load substantially. However, having 500 MW wave power in each MRE node could potentially alleviate 254.11 MW load loss on an hourly average basis, throughout the Western Interconnection.

4.5. Impact of wave energy integration during a heat wave scenario: 2020 California event

In this section, we investigate the impact of having different wave power capacities during the historical California heat wave (August 14th–August 19th, 2020). This event caused a considerable rise in LMPs throughout California due to higher electricity loads resulting from increased space cooling demands. Amidst this historical event, California Independent System Operator (CAISO) ordered rotation outages in California to preserve stability in bulk electricity grid operations [49].

Fig. 11 shows the nodal LMP effects of having wave power in the generation mix during the heat wave event. Integrating 100 MW wave power does not lead to a noticeable LMP drop. On the other hand, when the installed capacity of wave power at each MRE node increased to

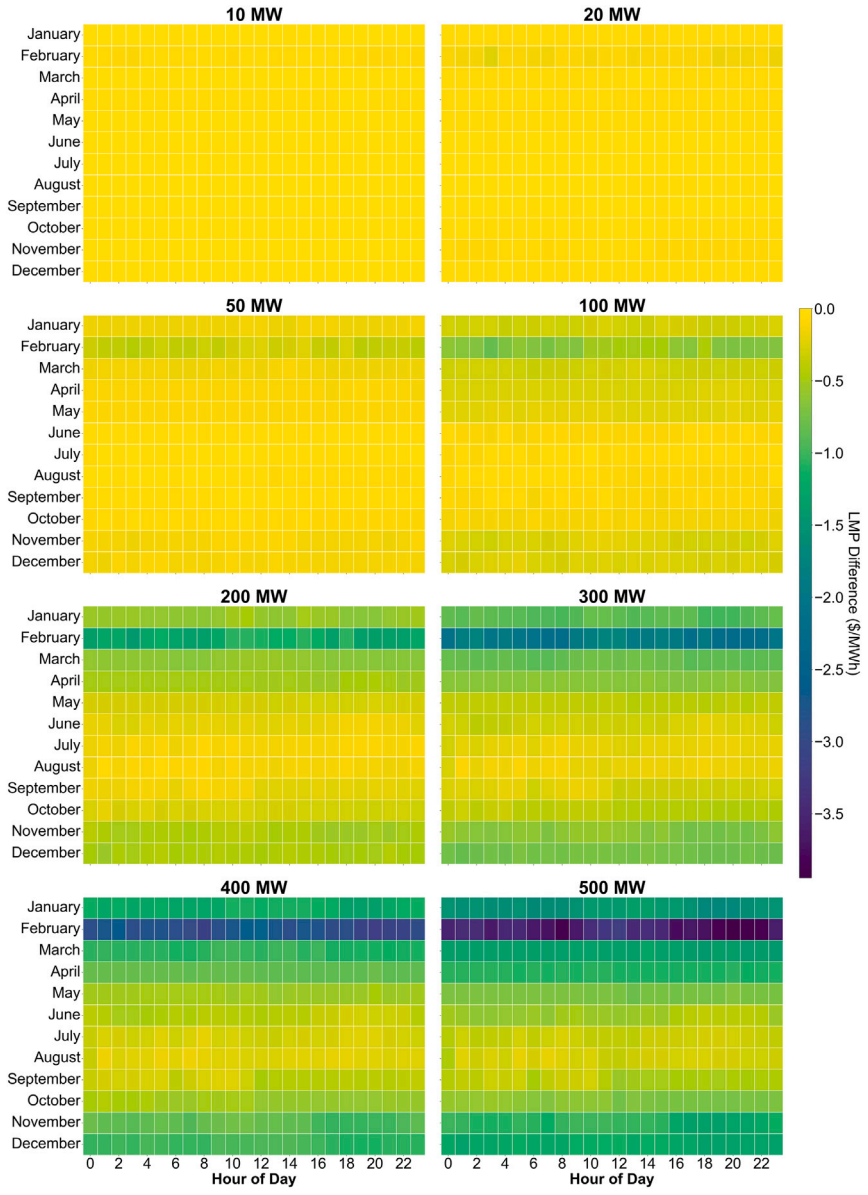

Fig. 7. Fluctuation map of LMP changes due to wave power integration for each scenario. LMP difference designates the change in LMPs between the baseline scenario (0 MW MRE) and each MRE scenario. Negative values show LMP decrease due to wave power integration. Each row shows the hourly profile of an average day in different months of 2019. In this figure, all transmission lines are scaled by +500 MW.

500 MW, we can see the nodal LMPs decrease to some extent. However, LMP depreciation is only localized to northern California (up to the Bay Area) due to the lack of transmission capacity to transmit low-cost wave power to southern California. Therefore, we can infer that concurrent transmission expansion is required to take full advantage of wave power during an extreme weather event like a heat wave.

When compared to the line contingency event discussed in Section 4.4, the severity of LMP spikes and loss of load events during the 2020 California heat wave is lower (see Fig. 12). Although 100 MW wave power capacity helped to reduce LMPs slightly, the positive impact of integrating 500 MW wave power is much more pronounced. During the 2020 California heat wave, integrating 100 MW and 500 MW wave power might have reduced the average hourly LMPs by 0.8 and 5.36 $/MWh. Wave power did not play a significant role in changing the minimum LMPs but 500 MW wave power could have alleviated maximum LMPs by 16.6 $/MWh. In addition, wave power help curb price volatility and increase reliability by decreasing the standard deviation of LMPs and total unserved load (see Table 4). However, a comparison of Fig. 12 with Fig. 10 reveals that the cost and reliability (i.e., LMP and loss of load) advantages of having wave energy through this heat wave are considerably lesser than the line contingency scenario in Section 4.4.

Finally, the share of wave power in the generation mix in California during the historical heat wave is presented in Fig. 13. Since wave power is more prominent during nighttime [12], its share in the generation mix is more observable during those periods. Nevertheless, wave power is present in the generation mix in varying amounts throughout the day. On a cumulative scale, during the heat wave event, 500 MW wave capacity installation in each MRE node constitutes ~1% of the total generation mix by replacing power generated from natural gas in California. The capacity of total wave power in California (2000 MW from 4 MRE nodes) corresponds to ~2.5% of the total installed capacity in California. Note that our analysis does not consider temperature-based deratings of thermal power plants. We believe that when integrated into the model, an additional temperature-based derating component in the operation of the thermal power plants would likely increase the benefit of wave power utilization during this heat wave [54]. However, a detailed analysis of temperature-based

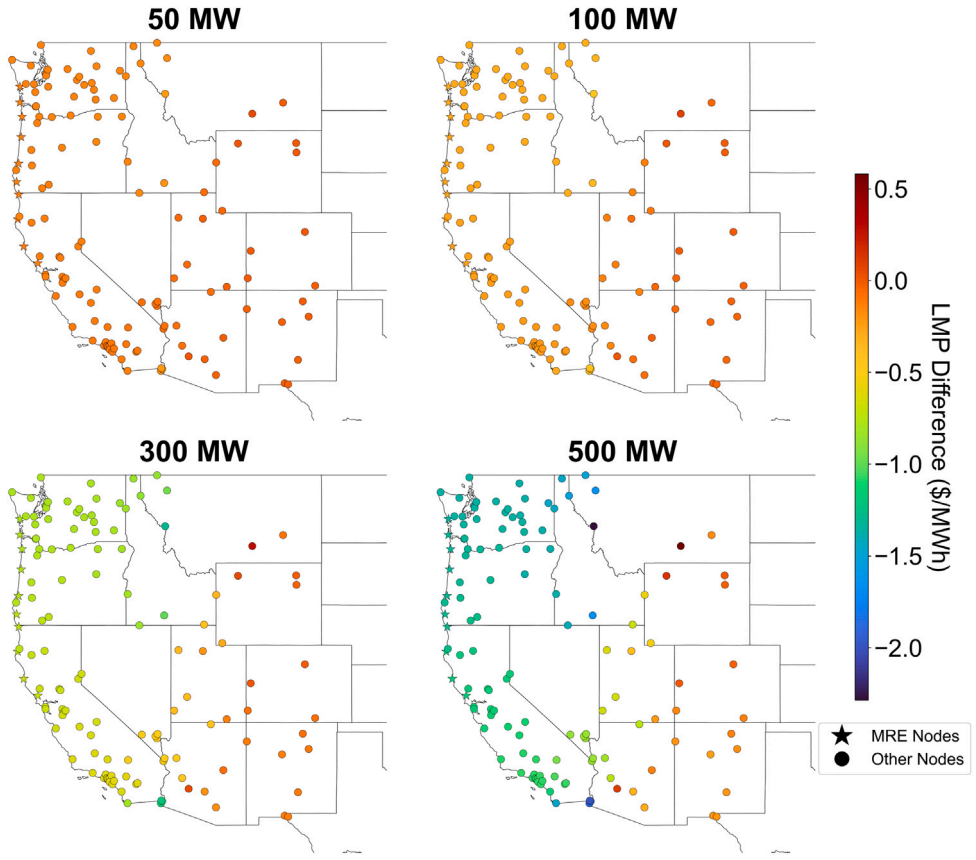

Fig. 8. Average nodal LMP changes due to wave energy integration for four selected scenarios in 2019. LMP difference designates the change in LMPs between the baseline scenario (0 MW wave energy capacity) and each wave integration scenario. Negative values show LMP decrease due to wave energy integration. Color designates the magnitude of average LMP change at each node. MRE nodes are shown with stars whereas other nodes are shown with circles. In this figure, all transmission lines are scaled by +500 MW.

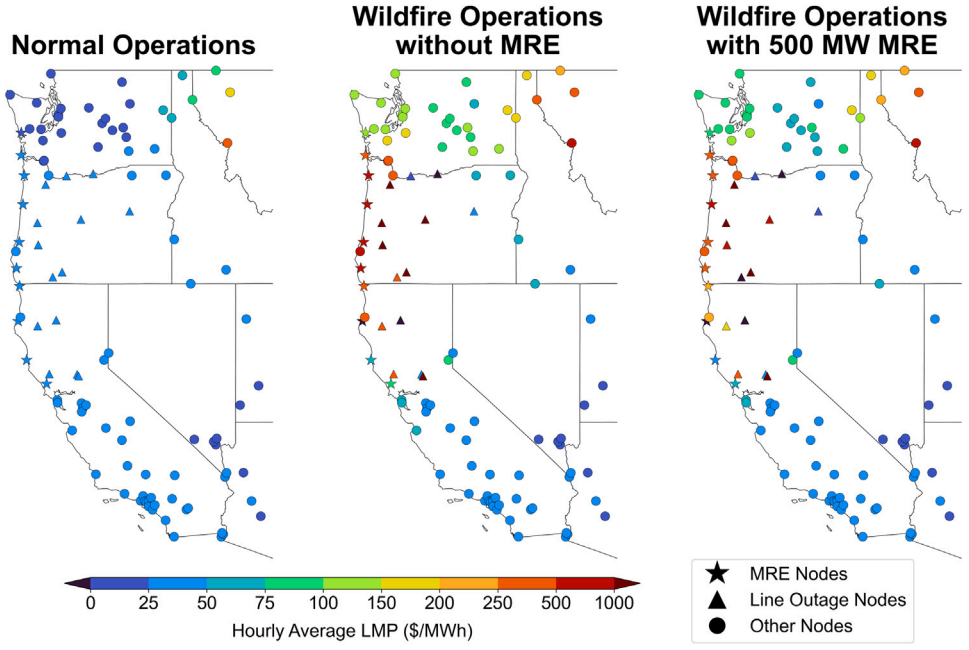

Fig. 9. (Left) Nodal LMPs without the artificial wildfire; (center) nodal LMPs with the artificial wildfire but no wave power integration; (right) nodal LMPs with the artificial wildfire and 500 MW wave power integration to every MRE node. The nonlinear color bar designates the average LMPs during the week of the hypothetical event. MRE nodes are shown with stars, nodes connected to lines on outage are shown with triangles, and other nodes are shown with circles.

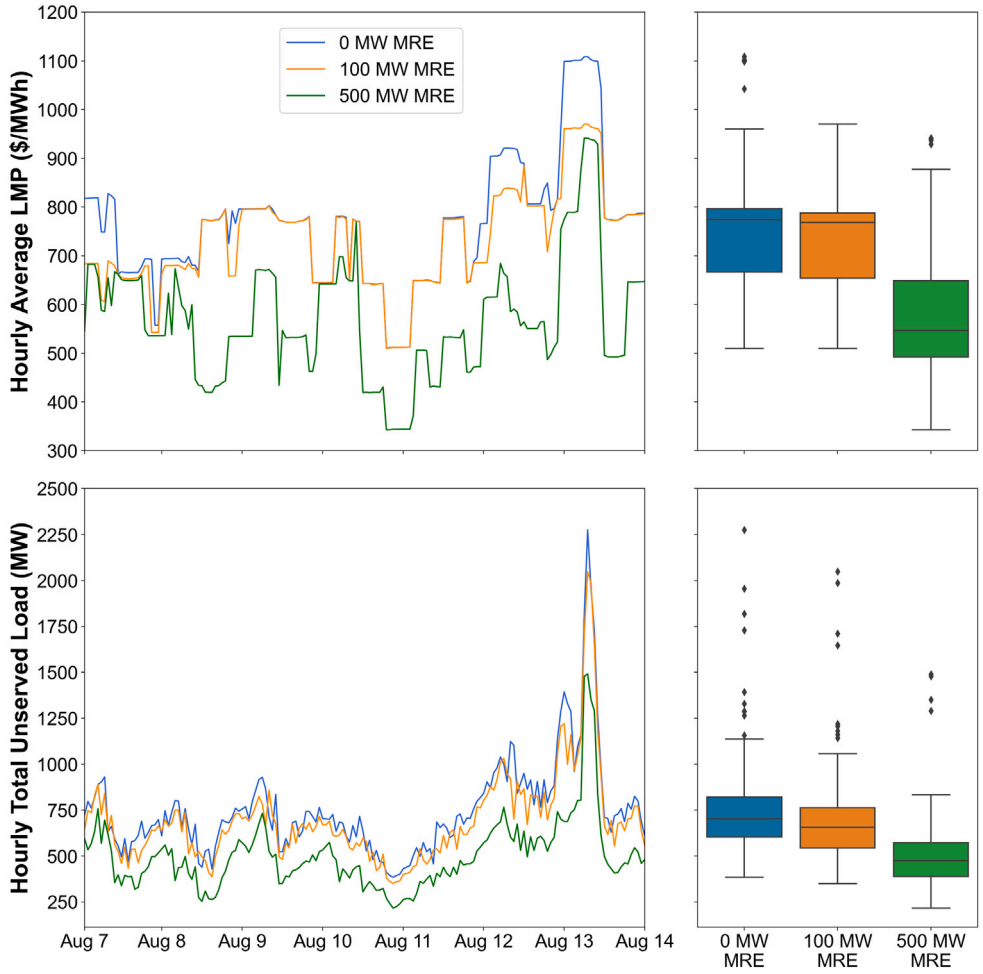

Fig. 10. (Top left) Hourly average LMP time series in line outage nodes; (top right) distribution of hourly average LMPs in line outage nodes; (bottom left) hourly total unserved load time series in line outage nodes; (bottom right) distribution of hourly total unserved load in line outage nodes. These results are focusing on the week of the hypothetical wildfire event. Colors designate the three MRE integration scenarios (0 MW MRE (baseline), 100 MW MRE, and 500 MW MRE).

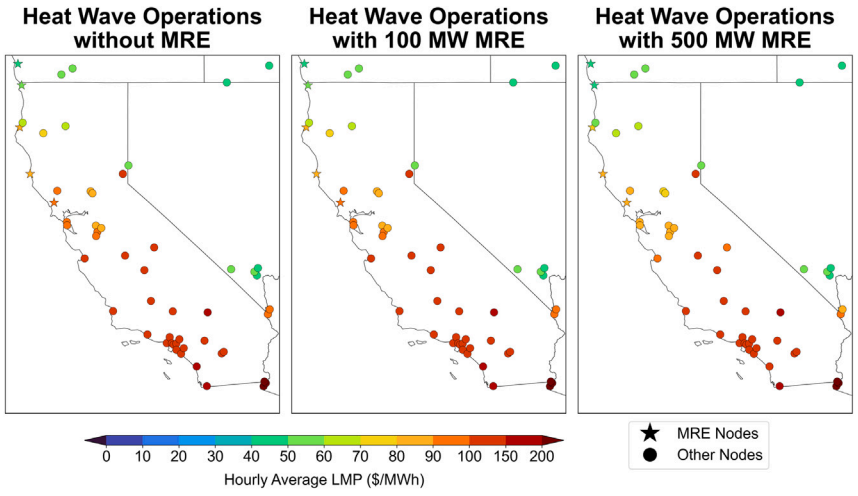

Fig. 11. (Left) hourly average LMPs during the heat wave without wave power integration; (middle) hourly average LMPs during the heat wave with 100 MW wave power integration; (right) hourly average LMPs during the heat wave with 500 MW wave power integration.

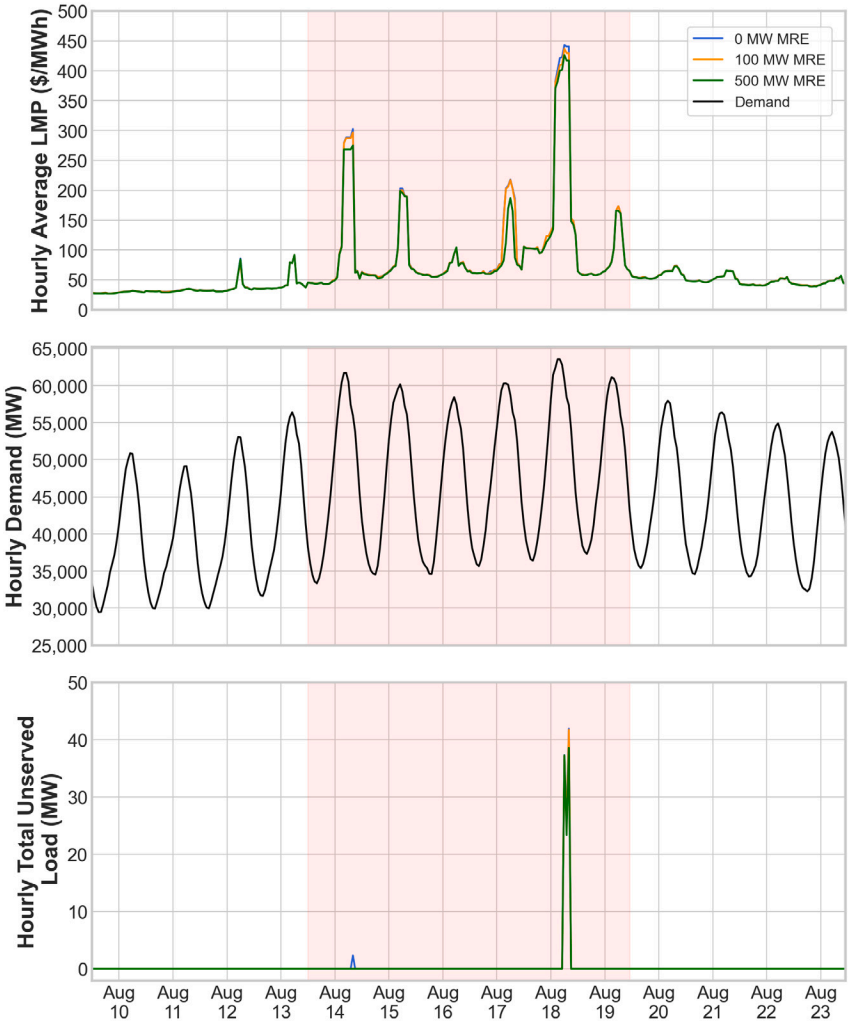

Fig. 12. (Top) hourly average LMP time series in California; (middle) hourly electricity demand time series in California; (bottom) hourly total unserved load time series in California. The duration of the heat wave is highlighted in red. Colors designate the three MRE integration scenarios (0 MW MRE (baseline), 100 MW MRE, and 500 MW MRE).

Table 4
Summary statistics for California during the heat wave event in 2020.

Scenario	Avg. LMP ($/MWh)	Std. Dev. of LMPs ($/MWh)	Max. LMP ($/MWh)	Min. LMP ($/MWh)	Total Hourly Unserved Load (MW)
No wave power + heat wave scenario	106.91	90.39	443.21	42.94	107.78
100 MW wave power + heat wave scenario	106.11	88.64	437.13	42.93	103.77
500 MW wave power + heat wave scenario	101.55	84.19	426.61	42.90	99.16

deratings of thermal power plants is beyond the scope of this current work and is deferred to future work.

5. Conclusion, limitation and future directions

In this paper, we performed a data-driven analysis to understand the impact of wave energy integration on power system operations for a bulk transmission grid. Specifically, a reduced topology network of the U.S. Western Interconnection was developed, to which wave generation was added at strategic points, to varying capacities. Our results indicated that beyond a threshold of ~100 MW of wave capacity in each of the MRE nodes, wave energy integration can bring down energy prices (LMPs), as well as reduce price volatility. Without widespread transmission infrastructure upgrades, the impact of wave generation is likely to remain geographically confined to the Pacific Northwest region (mainly Washington, Oregon, and northern parts of California). Our studies also indicate that concurrent transmission upgrades, along with wave energy integration are likely to aid a greater geographical spread of the benefits of wave energy integration. Finally, we studied the impact

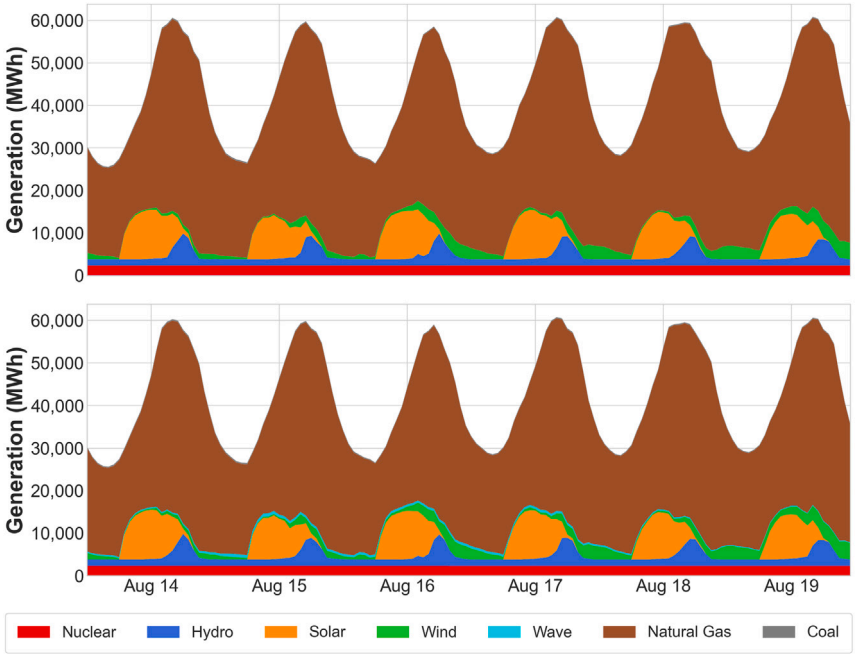

Fig. 13. (Top) hourly generation mix in California during the heat wave without wave power integration; (bottom) hourly generation mix in California during the heat wave with 500 MW wave capacity integration.

of wave generation during two resilience-driven events. In the first of these events, where we simulated a wildfire-driven transmission outage across a major transmission corridor, we observed that wave energy integration can enable price spike reduction by assuaging generation shortages, especially in nodes that are directly impacted by the outage events, and have sufficient transmission network connectivity to receive wave power benefits. In the second scenario, we studied the impacts of wave energy generation on grid operations during a heat wave event. The advantages of wave power were observed to be marginal in this case, likely due to wave being predominantly a winter peaking resource (while the heat wave happened in summer) and the impacted zone having limited connectivity to wave resources.

While several interesting operational insights were obtained through our studies, there are some limitations, and therefore, future research directions, which are discussed as follows. Firstly, this model assumes that the grid operator has perfect foresight and there are no forecast uncertainties (i.e., there are no errors in demand, solar, wind, and wave power forecasts). Moreover, we model only day-ahead market operations. Including real-time electricity markets with stochastic forecast errors would make the simulations more accurate; however, would steeply increase computation time and resource needs. Secondly, we consider one central operator for all balancing authorities within the selected model. In other words, one objective function represents coordination across all BAs *en masse*. Since the benefits of the wave energy-based generation resources are not shared equally among BAs, having different objective functions with an embedded economic investment model can help with analyzing the effects of wave energy resources in each individual BA. Finally, we assumed the same wave power capacity integrated into every wave generator (MRE) node. Deciding on different wave power capacities for each node by taking wave power density at each coastal node into consideration would increase the model's fidelity to the real-world decision-making process. Along with the aforementioned directions, future efforts will also probe similar research questions for other types of grids that have different demand patterns and resource availability (such as U.S. Eastern Interconnection) and other potential climate-driven resilience scenarios (such as winter storms).

6. Software and data availability

The model is open-source and publicly available. All codes of the model and data used are available under MIT free software license [55].

CRediT authorship contribution statement

Kerem Ziya Akdemir: Writing – original draft, Visualization, Validation, Software, Methodology, Investigation, Formal analysis, Data curation, Conceptualization. **Bryson Robertson:** Writing – original draft, Supervision, Resources, Investigation, Data curation, Conceptualization. **Konstantinos Oikonomou:** Writing – review & editing, Methodology, Formal analysis, Data curation. **Jordan Kern:** Writing – review & editing, Supervision, Software, Resources, Investigation, Formal analysis. **Nathalie Voisin:** Writing – review & editing, Resources, Investigation. **Sarmad Hanif:** Writing – review & editing, Project administration, Funding acquisition. **Saptarshi Bhattacharya:** Writing – original draft, Supervision, Project administration, Investigation, Funding acquisition, Formal analysis, Conceptualization.

Declaration of competing interest

The authors declare that they have no known competing financial interests or personal relationships that could have appeared to influence the work reported in this paper.

Data availability

Data will be made available on request.

Acknowledgments

This material is based upon work supported by the U.S. Department of Energy (DOE). Pacific Northwest National Laboratory is operated for the DOE by Battelle Memorial Institute under Contract DE-AC05-76RL01830.

References

[1] Hamid Ishfaq, Alam Md Shabbir, Kanwal Asma, Jena Pabitra Kumar, Murshed Muntasir, Alam Risana. Decarbonization pathways: The roles of foreign direct investments, governance, democracy, economic growth, and renewable energy transition. Environ Sci Pollut Res 2022;1–16.

[2] Arabzadeh Vahid, Mikkola Jani, Jasiūnas Justinas, Lund Peter D. Deep decarbonization of urban energy systems through renewable energy and sector-coupling flexibility strategies. J Environ Manag 2020;260:110090.

[3] Akdemir Kerem Ziya, Kern Jordan D, Lamontagne Jonathan. Assessing risks for New England's wholesale electricity market from wind power losses during extreme winter storms. Energy 2022;251:123886. http://dx.doi.org/10.1016/j.energy.2022.123886.

[4] Vargas Carlos A, Caracciolo Luca, Ball Philip J. Geothermal energy as a means to decarbonize the energy mix of megacities. Commun Earth Environ 2022;3(1):66.

[5] Moazzen Iman, Robertson Bryson, Wild Peter, Rowe Andrew, Buckham Bradley. Impacts of large-scale wave integration into a transmission-constrained grid. Renew Energy 2016;88:408–17.

[6] Fairley Iain, Smith Helen CM, Robertson Bryson, Abusara Mohammad, Masters Ian. Spatio-temporal variation in wave power and implications for electricity supply. Renew Energy 2017;114:154–65.

[7] Reikard Gordon, Robertson Bryson, Bidlot Jean-Raymond. Combining wave energy with wind and solar: Short-term forecasting. Renew Energy 2015;81:442–56.

[8] Barstow Stephen, Mørk Gunnar, Mollison Denis, Cruz João. The wave energy resource. In: Ocean wave energy: current status and future prespectives. Springer; 2008, p. 93–132.

[9] Jacobson Paul T, Hagerman George, Scott George. Mapping and assessment of the United States ocean wave energy resource. Tech. rep., Electric Power Research Institute; 2011.

[10] Lehmann Marcus, Karimpour Farid, Goudey Clifford A, Jacobson Paul T, Alam Mohammad-Reza. Ocean wave energy in the United States: Current status and future perspectives. Renew Sustain Energy Rev 2017;74:1300–13.

[11] Baldwin S, et al. Advancing clean electric power technologies, technology assessments. In: Quadrennial technology review—an assessment of energy technologies and research opportunities. p. 100–43.

[12] Bhattacharya Saptarshi, Pennock Shona, Robertson Bryson, Hanif Sarmad, Alam Md Jan E, Bhatnagar Dhruv, et al. Timing value of marine renewable energy resources for potential grid applications. Appl Energy 2021;299:117281. http://dx.doi.org/10.1016/j.apenergy.2021.117281.

[13] Fairley Iain, Lewis Matthew, Robertson Bryson, Hemer Mark, Masters Ian, Horrillo-Caraballo Jose, et al. Global wave resource classification and application to marine energy deployments. In: EGU general assembly conference abstracts. 2020, p. 8135.

[14] Soudan Bassel. Community-scale baseload generation from marine energy. Energy 2019;189:116134.

[15] Pennock Shona, Coles Daniel, Angeloudis Athanasios, Bhattacharya Saptarshi, Jeffrey Henry. Temporal complementarity of marine renewables with wind and solar generation: Implications for GB system benefits. Appl Energy 2022;319:119276.

[16] Armstrong Sara, Cotilla-Sanchez Eduardo, Kovaltchouk Thibaut. Assessing the impact of the grid-connected pacific marine energy center wave farm. IEEE Journal of Emerging and Selected Topics in Power Electronics 2015;3(4):1011–20.

[17] Göteman Malin, Giassi Marianna, Engström Jens, Isberg Jan. Advances and challenges in wave energy park optimization—A review. Front Energy Res 2020;8:26.

[18] Rasool Safdar, Muttaqi Kashem M, Sutanto Danny. Modelling of a wave-to-wire system for a wave farm and its response analysis against power quality and grid codes. Renew Energy 2020;162:2041–55.

[19] Said Hafiz Ahsan, Ringwood John V. Grid integration aspects of wave energy—Overview and perspectives. IET Renew Power Gener 2021;15(14):3045–64.

[20] Robertson Bryson, Bekker Jessica, Buckham Bradley. Renewable integration for remote communities: Comparative allowable cost analyses for hydro, solar and wave energy. Appl Energy 2020;264:114677.

[21] Lavidas George, Blok Kornelis. Shifting wave energy perceptions: The case for wave energy converter (WEC) feasibility at milder resources. Renew Energy 2021;170:1143–55.

[22] Xu Xinxin, Robertson Bryson, Buckham Bradley. A techno-economic approach to wave energy resource assessment and development site identification. Appl Energy 2020;260:114317.

[23] Reikard Gordon, Robertson Bryson, Bidlot Jean-Raymond. Wave energy worldwide: Simulating wave farms, forecasting, and calculating reserves. International Journal of Marine Energy 2017;17:156–85.

[24] Iglesias Gregorio, López Mario, Carballo Rodrigo, Castro Alberte, Fraguela José A, Frigaard Peter. Wave energy potential in Galicia (NW Spain). Renew Energy 2009;34(11):2323–33.

[25] Matthew Chris, Spataru Catalina. Scottish islands interconnections: Modelling the impacts on the UK electricity network of geographically diverse wind and marine energy. Energies 2021;14(11):3175.

[26] Jaramillo Ruben Dario, Garces Alejandro. Wave energy: Modeling and analysis of power grid integration. IEEE Latin Am Trans 2015;13(12):3863–72.

[27] Johnson Brandon, Cotilla-Sanchez Eduardo. Estimating the impact of ocean wave energy on power system reliability with a well-being approach. IET Renew Power Gener 2020;14(4):608–15.

[28] Halamay Douglas A, Brekken Ted KA, Simmons Asher, McArthur Shaun. Reserve requirement impacts of large-scale integration of wind, solar, and ocean wave power generation. IEEE Trans Sustain Energy 2011;2(3):321–8.

[29] Akdemir Kerem Ziya, Oikonomou Konstantinos, Kern Jordan D, Voisin Nathalie, Ssembatya Henry, Qian Jingwei. An open-source framework for balancing computational speed and fidelity in production cost models. SSRN 2023. http://dx.doi.org/10.2139/ssrn.4507380.

[30] Fairley Iain, Lewis Matthew, Robertson Bryson, Hemer Mark, Masters Ian, Horrillo-Caraballo Jose, et al. A classification system for global wave energy resources based on multivariate clustering. Appl Energy 2020;262:114515.

[31] Zheng Chong-wei. Dynamic self-adjusting classification for global wave energy resources under different requirements. Energy 2021;236:121525.

[32] WECC. The western interconnection. 2017, https://www.wecc.org/epubs/StateOfTheInterconnection/Pages/The-Western-Interconnection.aspx. [Accessed 7 March 2023].

[33] WECC. Resource portfolio. 2018, https://www.wecc.org/epubs/StateOfTheInterconnection/Pages/Resource-Portfolio.aspx. [Accessed 7 March 2023].

[34] Expósito Antonio Gómez, Ramos José Luis Martínez, Santos Jesus Riquelme. Slack bus selection to minimize the system power imbalance in load-flow studies. IEEE Trans Power Syst 2004;19(2):987–95.

[35] EIA. Hourly electric grid monitor. 2022, https://www.eia.gov/electricity/gridmonitor/dashboard/electric_overview/US48/US48. [Accessed 12 October 2022].

[36] EIA. Form EIA-923 detailed data with previous form data (EIA-906/920). 2022, https://www.eia.gov/electricity/data/eia923/. [Accessed 18 October 2022].

[37] Turner Sean WD, Voisin Nathalie, Nelson Kristian. Revised monthly energy generation estimates for 1,500 hydroelectric power plants in the United States. Sci Data 2022;9(1):675.

[38] Birchfield Adam B, Xu Ti, Gegner Kathleen M, Shetye Komal S, Overbye Thomas J. Grid structural characteristics as validation criteria for synthetic networks. IEEE Trans Power Syst 2017;32:3258–65. http://dx.doi.org/10.1109/TPWRS.2016.2616385.

[39] Electric Grid Test Case Repository. ACTIVSg10k: 10000-bus synthetic grid on footprint of western united states. 2017, https://electricgrids.engr.tamu.edu/electric-grid-test-cases/activsg10k/. [Accessed 16 September 2022].

[40] WECC. 2030 ADS pcm release notes. 2021, https://www.wecc.org/Reliability/2030ADS_PCM_ReleaseNotes_GV-V2.3_6-9-2021.pdf. [Accessed 22 October 2022].

[41] Yang Zhaoqing, García-Medina Gabriel, Wu Wei-Cheng, Wang Taiping. Characteristics and variability of the nearshore wave resource on the US West Coast. Energy 2020;203:117818.

[42] Jin Siya, Zheng Siming, Greaves Deborah. On the scalability of wave energy converters. Ocean Eng 2022;243:110212.

[43] Booij N, Holthuijsen LH, Ris RC. The "swan" wave model for shallow water. In: Coastal engineering 1996. 1996, p. 668–76.

[44] Robertson Bryson, Dunkle Gabrielle, Gadasi Jonah, Garcia-Medina Gabriel, Yang Zhaoqing. Holistic marine energy resource assessments: A wave and offshore wind perspective of metocean conditions. Renew Energy 2021;170:286–301.

[45] NREL. Marine energy atlas. 2021, https://maps.nrel.gov/marine-energy-atlas. [Accessed 27 November 2022].

[46] Robertson Bryson, Bailey Helen, Leary Matthew, Buckham Bradley. A methodology for architecture agnostic and time flexible representations of wave energy converter performance. Appl Energy 2021;287:116588.

[47] Tapia Tomas, Lorca Alvaro, Olivares Daniel, Negrete-Pincetic Matias, et al. A robust decision-support method based on optimization and simulation for wildfire resilience in highly renewable power systems. European J Oper Res 2021;294(2):723–33.

[48] Zanocco Chad, Stelmach Greg, Giordono Leanne, Flora June, Boudet Hilary. Poor air quality during wildfires related to support for public safety power shutoffs. Soc Nat Resour 2022;1–15.

[49] CAISO. Final root cause analysis: Mid-august 2020 extreme heat wave. 2021, http://www.caiso.com/Documents/Final-Root-Cause-Analysis-Mid-August-2020-Extreme-Heat-Wave.pdf. [Accessed 10 January 2023].

[50] EIA. Pacific northwest sees highest daily natural gas spot prices in the U.S. since 2014. 2019, https://www.eia.gov/todayinenergy/detail.php?id=38932. [Accessed 22 January 2023].

[51] Hoover Katie, Hanson Laura A. Wildfire statistics. Tech. rep., Congressional Research Service; 2021.

[52] Center National Interagency Fire. InterAgency fire perimeter history all years view. 2022, https://data-nifc.opendata.arcgis.com/datasets/nifc::interagencyfireperimeterhistory-all-years-view/explore?location=41.667952%2C-122.217971%2C8.72. [Accessed 23 January 2023].

[53] NOAA. Local climatological data station details: MONTAGUE siskiyou AIRPORT, CA US. 2023, https://www.ncdc.noaa.gov/cdo-web/datasets/LCD/stations/WBAN:24259/detail. [Accessed 23 January 2023].

[54] Dyreson A, Devineni N, Turner SWD, De Silva M. T, Miara A, Voisin N, et al. The role of regional connections in planning for future power system operations under climate extremes. Earth's Future 2022;10. http://dx.doi.org/10.1029/2021EF002554.

[55] Akdemir Kerem Ziya, Oikonomou Konstantinos, Kern Jordan D, Bhattacharya Saptarshi. GO WEST MRE impacts. 2023, https://github.com/keremakdemir/GO_WEST_MRE_Impacts/tree/Selective_line_scaling. [Accessed 18 April 2023].